Evidence for substrate assisted catalysis in *N*-acetylphosphoglucosamine mutase

Olawale G. Raimi[+], Ramon Hurtado-Guerrero[1,+], and Daan M. F. van Aalten*

Division of Gene Regulation and Expression, School of Life Sciences, University of Dundee, DD1 5EH, Scotland, UK

[1]Present address: Institute of Biocomputation and Physics of Complex Systems (BIFI), University of Zaragoza. BIFI-IQFR (CSIC) Joint Unit, Mariano Esquillor s/n, Campus Rio Ebro, Edificio I+D; Fundacion ARAID, Zaragoza, SPAIN

* To whom correspondence should be addressed: dmfvanaalten@dundee.ac.uk

+ These authors contributed equally to this work

ABSTRACT

N-acetylphosphoglucosamine mutase (AGM1) is a key component of the hexosamine biosynthetic pathway that produces UDP-GlcNAc, an essential precursor for a wide range of glycans in eukaryotes. AGM belongs to the α-D-phosphohexomutase metalloenzyme superfamily and catalyses the interconversion of *N*-acetylglucosamine-6-phosphate (GlcNAc-6P) to *N*-acetylglucosamine-1-phosphate (GlcNAc-1P) through *N*-acetylglucosamine-1,6-bisphosphate (GlcNAc-1,6-bisP) as the catalytic intermediate. Although there is an understanding of the phosphoserine-dependent catalytic mechanism at enzymatic and structural level, the identity of the requisite catalytic base in AGM1/phosphoglucomutases is as yet unknown. Here we present crystal structures of a Michaelis complex of AGM1 with GlcNAc-6P and Mg^{2+}, and a complex of the inactive Ser69Ala mutant together with glucose-1,6-bisphosphate (Glc-1,6-bisP) that represent key snapshots along the reaction coordinate. Together with mutagenesis, these structures reveal that the phosphate group of the hexose-1,6-bisP intermediate may act as the catalytic base.

INTRODUCTION

N-acetylphosphoglucosamine mutase (AGM1) catalyses the interconversion of *N*-acetylglucosamine-6-phosphate (GlcNAc-6P) to *N*-acetylglucosamine-1-phosphate (GlcNAc-1P) in eukaryotes [1]. This enzyme is a member of the α-D-phosphohexomutase superfamily of enzymes that catalyse intramolecular phosphoryl transfer on a range of phosphosugar substrates [2]. The reaction catalyzed by AGM1 is the third step in the biosynthesis of UDP-GlcNAc from fructose-6-phosphate in the hexosamine pathway [3]. UDP-GlcNAc is an important metabolite for a number of cellular processes. In bacteria, it is the precursor of outer membrane lipopolysaccharide [4, 5] and cell wall peptidoglycan [6]. In eukaryotes, it is the precursor of GPI anchors [7] together with its role as sugar donor in a number of glycosylation reactions including *N*-glycosylation and *O*-glycosylation [8, 9]. In fungi, UDP-GlcNAc is also the precursor of chitin and mannoproteins, which are essential components of the fungal cell wall [3]. Knock out of any of the genes encoding enzymes of the UDP-GlcNAc pathway has been demonstrated to be lethal in *Saccharomyces cerevisiae*, unless exogenous glucosamine or *N*-acetylglucosamine is available [1, 10, 11]. Recently, AGM1 was shown to be an essential gene in the human fungal pathogen *Aspergillus fumigatus* and has been proposed as a drug target [12]. However, there are no mechanism-inspired inhibitors of this family of enzymes due to a limited understanding of their catalytic mechanisms.

The phosphohexomutase superfamily comprises two subfamilies separated by their ability to operate on α-D-sugar 1-phosphates or β-D-sugar 1-phosphates. While the former family is distinguished by the phosphorylation of a conserved serine to give a stable phosphate monoester [2], the latter uses a conserved aspartate as a nucleophile to form a transient phospho-enzyme intermediate [13]. Some members of the phosphohexomutase superfamily, phosphoglucomutases, bacterial phosphoglucosamine mutases and yeast phosphoacetylglucosamine mutases share the common sequence motif Ser/Thr-X-Ser-His-Asn-Pro [14, 15]. Phosphorylation of these enzymes, shown to occur on the serine at the third position in the sequence motif [16], is required for full activity; however, the enzymes are initially produced in an inactive, dephosphorylated form [17]. A hexose-1,6-bisphosphate has been reported to be the phosphate donor in the activation process during catalysis that occurs via a ping-pong bi-bi mechanism [14, 16, 18]. It has also been shown that the phosphoglucosamine mutase from *Escherichia coli* autophosphorylates *in vitro* in the presence of [^{32}P]ATP and the same was observed for phosphoglucosamine mutases from

other bacterial species, yeast *N*-acetylglucosamine-phosphate mutase, and rabbit muscle phosphoglucomutase [17]. Several crystal structures complexed with phosphate mimics (e.g. trifluoromagnesate "MgF_3^-" and trifluoroberrylate "BeF_3^-") or phosphate together with phosphosugars have revealed the residues implicated in substrate binding and catalysis, and revealed large conformational changes [2, 13, 19]. However, the identity of the catalytic base for these enzymes is as yet unknown.

Here, we describe the crystallographic snapshots of *A. fumigatus* AGM1 (*Af*AGM1) that reveal large conformational changes accompanying phosphoryl transfer. Furthermore, the complexes, together with modelling studies, suggest that the phosphate group of the reaction intermediate may act as the catalytic base during catalysis. This increase in understanding of the reaction mechanism of this class of enzymes could be exploited in the rational design of mechanism-inspired inhibitors.

MATERIALS AND METHODS

Mutagenesis

The previously published *Af*AGM1 GST fusion construct, pGEX-6P *Af*AGM1 [12], served as the template for the generation of S69A and S507A amino-acid substitutions by site-directed mutagenesis, using the mutagenic oligonucleotides 5´-GGATTGGCGTCATGGTCACTGCGGCTCATAATCCTGCCGAGGACAATGG-3´ (S69A forward), 5´-CCATTGTCCTCGGCAGGATTATGAGCCGCAGTGACCATGACGCCAATCC-3´ (S69A reverse), 5´-GGGACGAAGCTTCGCTCGTGCAG7CTGGCACGGAAGATGCGGTGCGTG-3´ (S507A forward) and 5´-CACGCACCGCATCTTCCGTGCCAGCTGCACGAGCGAAGCTTCGTCCC-3´ (S507A reverse). Site-directed mutagenesis was carried out following the QuickChange Site-Directed Mutagenesis protocol (Stratagene), using the KOD HotStart DNA polymerase (Novagene). All plasmids were verified by sequencing using the University of Dundee sequencing service.

Protein production and purification

*Af*AGM1 and mutated forms were produced and purified as described previously [12]. Briefly, the *E. coli* strain BL21 (DE3) pLysS was used to produce the proteins and the purification consisted of chromatographic steps, with glutathione Sepharose 4B beads and a Superdex75 gel filtration column (2.6 x 60 cm) (Amersham Biosciences). Prior to gel filtration, the GST from the fusion protein was cleaved by PreScission protease.

Crystallization, data collection and structure determination

Crystals of the wild type enzyme were grown in a mother liquor containing 20 % PEG 1000, 100 mM HEPES, pH 7.25, as described previously [12]. The complex with GlcNAc-6P was obtained by soaking experiments with the sugar and an excess of $MgCl_2$. Crystals of the *Af*AGM1_S69A mutant co-crystallised with 15 mM Glc-1,6-bisP and 5 mM $MgCl_2$ were obtained in several conditions: 0.2 M sodium thiocyanate, 20% PEG 3350 and 0.1 M sodium bromide; 0.10 M glycine, 22% PEG 3350 and 0.2 M sodium thiocyanate; and a final condition with 0.16 M glycine, 16% PEG 3350 and 0.2 M sodium thiocyanate. The two complexes crystallised after 2 - 3 days in the space group $P2_12_12_1$ with differences in the unit cell

dimensions with respect to the wild type (Table I). X-ray diffraction data were collected at the BM14 beam line of the European Synchrotron Radiation Facility (ESRF, Grenoble, France). Single crystals were cryoprotected (15 % glycerol plus the appropriate mother liquor) and frozen in a nitrogen gas cooled to 100 K. Complete data sets were collected for the GlcNAc-6P and Glc-1,6-bisP complexes. Data were processed with HKL2000 [20]. Both complexes were solved by molecular replacement using a previously described structure of the wild type enzyme in complex with magnesium [12]. Refinement was performed with REFMAC5 [21] and model building with COOT [22]. Ligand structures and topologies were generated by PRODRG [23]. Models for ligands were not included until their conformations were completely defined by unbiased $|F_o| - |F_c|$, φ_{calc} electron density maps. Pictures were generated using Pymol [24].

Enzyme kinetics

To determine the phosphoglucose mutase and phophoglucosamine mutase activities of AGM1, three different coupled assays were carried out (Figure 1). Assay A was carried out in the presence of glucose-6P dehydrogenase (G6PDH) with or without Glc-1,6-bisP as cofactor using glucose-1P (Glc-1P) as the substrate. This assay was carried out in a 100 µl reaction volume containing 50 mM MOPS pH 7.4, 1.5 mM $MgSO_4$, 1 mM DTT (dithiothreitol), a range of Glc-1P concentrations, 1 mM NAD^+ and 0.01 units of G6PDH (Sigma). The reaction was started by the addition of 10 nM *Af*AGM1 and incubated for 60 min at 20 °C. The amount of NADH produced was measured using a fluorescence reader (FL×800). Assay B was done in the presence of UDP-N-acetylglucosamine pyrophosphorylase (UAP1) as the coupled enzyme using GlcNAc-6P as the substrate as described [12]. The reaction mixture (100 µl) contained 50 mM MOPS pH 7.4, 1.5 mM $MgSO_4$, 250 µM UTP, varying concentrations of GlcNAc-6P (2.5–300 µM), 100 nM *Af*AGM1, 0.5 µM *Af*UAP1 and 0.04 units pyrophosphatase (Sigma) to convert the *Af*UAP1 reaction product inorganic pyrophosphate (PPi) to inorganic phosphate (Pi). The reaction was incubated at 20 °C for 30 min and terminated by the addition of 100 µl Biomol green (0.03% (w/v) malachite green, 0.2% (w/v) ammonium molybdate and 0.5% (v/v) Triton X-100 in 0.7 N HCl) and left for a further 20 min at 20 °C for colour development. Absorbance at 620 nm was read using a spectrophotometer. Assay C involves coupling with UDP-glucose pyrophosphorylase using glucose-6P(Glc-6P) as the substrate and the Biomol green assay as described earlier [12, 25].

*Modelling and energy minimization of Af*AGM1_*S69A mutant-Glc-1,6-bisP complex*

To generate a model of the complex of *Af*AGM1 with Glc-1,6-bisP, the *Af*AGM1_S69A-Glc-1,6-bisP mutant complex crystal structure was used as a template. Using COOT, the Ala69 in *Af*AGM1_S69A mutant was mutated to the original Ser69 and a rotamer of Asp288 was chosen to allow coordination of the magnesium as found in the wild-type structure with Mg^{2+} and GlcNAc-6P (see below). Magnesium was also incorporated in COOT after superposition with the wild-type structure with Mg^{2+} and GlcNAc-6P complex and energy minimization was performed using Schrödinger software [26]. The crystal structure was read with the Maestro program [27], and the Protein Preparation Wizard module was used to add hydrogens, assign correct bond orders, and solve steric conflicts. Once the structure was prepared, a partial minimization of hydrogen atoms was initially performed by means of the Impact Refinement module, using the OPLS-2005 force field [27] and finished when RMSD (root mean square deviation) reached a maximum cut-off of 0.3 Å. After this initial minimization, a further total minimization including heavy atoms was also made using the same conditions and terminated with an RMSD of 0.10 Å with respect to the original *Af*AGM1_S69A mutant-Glc-1,6-bisP complex.

RESULTS AND DISCUSSION

Ser69 is the AfAGM1 catalytic serine

Previously we identified pSer69 as the potential catalytic residue in *Af*AGM1 by mass-spectrometry (MS/MS), phosphosite mapping and crystallographic studies of the wild type enzyme in complex with magnesium [12]. To further explore the role of the *Af*AGM1_pSer69 in catalysis, we determined steady state kinetics with different substrates in the absence and presence of Glc-1,6-bisP as the activator. The wild type enzyme demonstrated both *N*-acetylphosphoglucosamine and phosphoglucose mutase activity with K_ms of 25 μM for its native substrate GlcNAc-6P, 300 μM for Glc-6P and 1.2 mM for Glc-1P (Table II), demonstrating that the enzyme specifically recognises the *N*-acetyl group. We also determined the crystal structure of *Af*AGM1 in complex with GlcNAc-6P and magnesium (Table I), showing the typical four domains forming a heart shape found previously for other members (domain 1 to 4, Figures 2A and 2B). Domain 1 (residues 1-187), 2 (residues 188-305), 3 (residues 306-442), and 4 (residues 443-542) bear the predicted active serine loop, the metal-binding loop, the sugar-binding loop and the phosphate-binding, respectively. The overall structure of this enzyme is similar to that of *Candida albicans N*-acetylphosphoglucosamine mutase (*Ca*AGM1) [2] (52% sequence identity, RMSD of 1.2 Å on 496 Cα atoms) and the *Pseudomonas aeruginosa* phosphomannomutase/phosphoglucomutase *(Pa*PMM/PGM) [28] (20% sequence identity and RMSD of 2.3 Å on 343 Cα atoms). At the active site of one of the two monomers in the asymmetric unit, unambiguous electron density defining a phosphorylated Ser (Ser69) was present (Figure 3A). The conformation of the phosphoserine with a O…..P-O angle of 158^o would facilitate inline attack/displacement by the GlcNAc-6P O1 and hence further supports the role of this residue as the phosphoryl donor/acceptor (Figure 3A).

To further verify the role of S69 as the phosphoryl donor/acceptor, the S69A *Af*AGM1 mutant was investigated. As expected, steady-state kinetics (Table II) reveal that mutating Ser69 to alanine completely abolishes enzyme activity. A similar study of human AGM1 also reported a complete loss of activity when the equivalent Ser64 was mutated to alanine or threonine [29]. Interestingly, in a study of an equivalent mutant (Ser108Ala) in *Pa*PMM/PGM, another member of the same phosphohexomutase superfamily [30, 31], some residual activity was reported [31]. It was proposed that this might be the result of another residue in the active site being phosphorylated in the absence of Ser108 [30]. We noted the proximity of

Ser507 to the substrate-binding site, located in the phosphate-binding loop (Figure 3). However, mutating the *Af*AGM1 S507 to alanine does not significantly affect activity (Table II) suggesting that this serine does not contribute to catalysis. Thus, Ser69 is the *Af*AGM1 catalytic serine.

Phosphoryl transfer is associated with large conformational changes

Once it was clarified that Ser69 was the only residue being phosphorylated during catalysis, we exploited this catalytically impaired mutant to trap the bisphosphorylated intermediate that has been proposed for this class of phosphomutase [30] (Figure 3). The protein was crystallized with Glc-1,6-bisP and the structure was refined to 1.9 Å resolution with a single protein molecule in the asymmetric unit (Table I). The overall structure of *Af*AGM1_S69A-Glc-1,6-bisP complex shows a closed conformation, compared to the open/semi-open conformations exhibited by the two monomers in the *Af*AGM1-GlcNAc-6P-Mg^{+2} complex (Figure 2B). Together, these complexes reveal overall conformational changes accompanying phosphoryl transfer. Superposition of the opened and semi-opened conformations yields an RMSD of 0.76 Å with the loop on domain 4 moving 1.4 Å towards the active site cleft (Supplementary Figure 1). Superposition of the semi-opened and closed conformations yields an RMSD of 2.1 Å with the loops on domains 1 and 4 moving 2.0 and 3.4 Å, respectively. Superposition of the opened and closed conformations yields an RMSD of 2.3 Å with the loop on domain 4 moving 4.0 Å while the loop on domain 1 is disordered in the opened conformation structure (Supplementary Figure 1). Thus, domain 4 of the enzyme appears to be mobile, closing or opening the active site in response to interactions between the enzyme and its substrates/products/intermediate. We have visualised this with a video that has been included in the supplementary material (Supplementary Figure 2). The dephospho-*Af*AGM1-GlcNAc-6P complex has an overall structure with an open active site (Figure 2B) and may represent the inactive enzyme or ‘apo’ like conformation. This complex provides the likely snapshot of the conformation of the protein just before the first phosphoryl transfer or the release of product from the active site. However, the inactive *Af*AGM1_S69A mutant-Glc-1,6-bisphosphate complex has an overall structure with a closed active site (Figure 2B) and represents the reaction intermediate with Glc-1,6-bisphosphate buried in the active pocket. This is the first crystallographic evidence of the structural changes by this class of enzymes during catalysis, which corroborates the reaction mechanism proposed by Regni *et al.* [28]. The complete closure of the active site is achieved by the establishment of extensive

hydrogen bond interactions between the reaction intermediate Glc-1,6-bisphosphate and the protein (Figure 3). While the 1-phosphate group of the ligand pointing to Ala69 occupies partly the position of the phosphoserine observed in the *Af*AGM1_S69A-Glc-1,6-bisP complex, the 6-phosphate group is located in the phosphate-binding domain. In addition, the 1-phosphate group establishes hydrogen bond interactions with R33, H70, R289 and a water molecule, the 6-phosphate group makes hydrogen bond interactions with T29, R505, S507, T509, R514 and the backbone of G508, and the 3-OH and 4-OH groups of the sugar make hydrogen bond interactions with E380 and the backbone of V363 (Figure 3). Thus, extensive hydrogen bond interactions are established with residues from all the domains resulting in a closed conformation (Figure 2B). This provides a snapshot of the reaction either immediately after phosphoryl transfer to form the intermediate or before the second phosphoryl transfer to re-phosphorylate the enzyme. The phospho-*Af*AGM1-GlcNAc-6P-Mg^{2+} Michaelis complex reveals a semi-opened active site and may represent the active complex. For this complex, it was observed that GlcNAc-6P made hydrogen bond interactions with residues R505, R514, S507, T509, G508, E380 and V363 from domains 3 and 4 of the protein but not with any residues from domains 1 and 2. Furthermore, the *Af*AGM1_pSer69 establishes hydrogen bond interactions with residues R33, R289 and H70 from domains 1 and 2 as well as Mg^{2+}, which is coordinated by D288, D284 and D286 (Figure 3), hence domains 3 and 4 relax to open the active site cleft (Figure 2B). Although these interactions are different from the previously determined *Ca*AGM1-GlcNAc-6P-Zn^{2+}-P or *Ca*AGM1-GlcNAc-1P-Zn^{2+}–P complex [2] which shows extensive hydrogen bond interactions with residues from all the domains (Figure 3), the phospho-*Af*AGM1-GlcNAc-6P-Mg^{2+} complex may represent a snapshot of the conformation that supports the proposed reorientation of the intermediate or conformation just before the first phosphoryl transfer (Figure 2B). It is likely that for the reorientation of the intermediate to occur, the domains have to be relaxed from the closed state to the semi-open conformation (Figure 2B) allowing the reorientation of the intermediate without leaving the enzyme active site. In summary, these structures reveal that phosphoryl transfer is associated with large conformational changes.

The catalytic role of Ser69 depends on its coordination to a magnesium ion

AGM belongs to the α-D-phosphohexomutase metalloenzyme superfamily and the magnesium ion is essential for catalysis [16]. Structures of related phosphohexomutases in complex with substrates/products or the bisphosphosugar intermediate have been described, but they have not provided a detailed understanding of the atomic trajectories during catalysis [28, 32]. In this work, we have obtained two different complexes that represent distinct steps of the catalytic cycle. At the active site level, both pSer69 and phosphate group, either present in Glc-1,6-bisP or as a free phosphate in *Candida albicans N*-acetylphosphoglucosamine mutase (*Ca*AGM1) [2], interact by electrostatic interactions and hydrogen bonds with conserved residues such as Arg33, His70, Arg289 and H384 (Figure 3; in *Ca*AGM1 these residues correspond to Arg30, His67, Arg295 and His391 respectively). His384 (His391 in *Ca*AGM1) is the only residue adopting on and off conformations that supports the concept of "near attack conformers (NACs)" present in other members of this superfamily [13]. These conformers exist to avoid repulsion among highly charged residues and consequently to optimize catalytic turnover [13]. In the case of AGM1, this histidine may switch from an off to an on conformation to activate the O-1 hydroxyl group of the GlcNAc-6P that would subsequently attack the phosphate atom (Figure 3). Furthermore, the phosphate group is coordinated either by a magnesium ion (see the phospho-*Af*AGM1-GlcNAc-6P-Mg^{2+} complex in Figure 3), which is needed in turn to have an active enzyme, or a zinc ion acting as an AGM1 inhibitor (see the *Ca*AGM1-ligand complexes in Figure 3) [2]. In *Af*AGM1, the magnesium ion is pentagonally coordinated in a square pyramidal arrangement by *Af*AGM1_pSer69, Asp284, Asp286 and Asp288 (Figure 3). This type of coordination has also been described for the structure of *Ca*AGM1 complexed with either GlcNAc-1P or GlcNAc-6P and zinc acting as an inhibitor (Figure 3) [2]. Although the inactive *Af*AGM1_S69A mutant-Glc-1,6-bisphosphate complex was crystallized in the presence of 10 mM $MgCl_2$, the structure (Figure 3) reveals absence of this metal and presence of a water molecule instead (Figure 3). The magnesium ion helps to stabilise the charges and hence facilitates the transfer of phosphoryl group between the *Af*AGM1_pSer69 and the O1 or O6 of the substrates [2, 33]. The catalytic serine is however key in the coordination to the magnesium ion throughout the catalytic cycle and therefore constitutes an essential feature for having a functional AGM1.

The phosphate group as the putative catalytic base

Previous work on pSer-dependent phosphohexomutases combined with the two new structures shown in this study do identify the amino acids that may be required for activation of the O1/O6 hydroxyls groups. Inspection of some of the amino acids interacting with the phosphoserine, the Glc-1,6-bisP or the free phosphate present in the *C. albicans* AGM1[2] reveals a number of candidates that may fulfil this role. For instance, His70 or His384 and Arg33 that form hydrogen bond interactions with 1P group of Glc-1,6-bisP and phosphate group of *Af*AGM1_pSer69 (Figure 3) could act as activators. Another alternative is that both the hydroxyl group from Ser69, and the O1/O6 hydroxyls from GlcNAc-1P/6P act as a nucleophile in the absence of a catalytic base, although this is unlikely given the proximity of the positive charge on the magnesium ion. To further explore this, we made a model of the wild type enzyme complexed with magnesium and Glc-1,6-bisP based on the structure of the inactive mutant reported here (Figure 4A). The template was used because it approximates the reaction intermediate catalytic step (Figure 3). Interestingly this model suggests that the phosphates may uptake the proton from the hydroxyl group of Ser69 leading to an increase of nucleophilicity of the serine side chain that is required to attack the phosphate. One of the pK_as of this phosphate group is ~ 6.8 which makes it compatible with its potential role as a catalytic base and further supports the proposed mechanism (Figure 4B). In this scenario GlcNAc-6P enters the active site and the oxyanion of 1-hydroxyl from GlcNAc-6P is precisely formed once it's located in front of *Af*AGM1_pSer69 by proton uptake by the phosphate group. In this manner, negative repulsion of the substrate and *Af*AGM1_pSer69 would be avoided and the reaction will only take place when both are correctly positioned. GlcNAc-1,6-bisP would be formed and the required flip over around the O5-C3 axis will render the 6-phosphate group in a position to be transferred to Ser69 by the same mechanism proposed (Figure 4B). Finally, GlcNAc-1P is formed, completing the catalytic cycle.

CONCLUSIONS

N-acetylphosphoglucosamine mutase is a key enzyme of the hexosamine biosynthetic pathway in eukaryotes. The enzyme catalyzes the inter-conversion of GlcNAc-6P to GlcNAc-1P, which is subsequently converted to UDP-GlcNAc by UDP-GlcNAc pyrophosphorylase, the last enzyme in the pathway. UDP-GlcNAc is the direct precursor for a number of cellular processes, for instance in fungi it is used in the synthesis of chitin that forms the major component of the fungi cell wall and it is thus believed that enzymes involved in its synthesis are potential drug targets [3, 34, 35]. The results presented here have helped our understanding of the catalytic mechanism of *Af*AGM1 and the wider phosphohexomutase superfamily. *Af*AGM1 shares the same overall structure with other members of this superfamily although its more similar to *Ca*AGM1[2] (RMSD 1.2 Å) than to phosphomannomutase/phosphoglucomutase (RMSD 2.3 Å). Although the crystal structure of the well-characterized member of the phosphohexomutase superfamily *Pa*PMM/PGM with phosphorylated active Ser108 has been reported, here we describe the first crystal structure of a member of the phosphoacetylglucosamine mutase subfamily with phosphorylated active Ser69 (Figure 2A). This posttranslational modification occurs during expression in *E. coli* by an as yet unknown mechanism which may involve autophosphorylation in the presence of ATP [17]. The kinetic characterization of the enzyme reveals that the enzyme possesses both phosphoglucomutase and phosphoacetylglucosamine mutase activity. The enzyme is capable of inter-converting Glc-1P to Glc-6P, GlcNAc-6P to GlcNAc-1P and Glc-6P back to Glc-1P but with different rate constants and GlcNAc-6P as the preferred substrate (Table II). The structural complexes described in this study reveal that depending on the catalytic cycle, the enzyme adopts conformational changes. Thus, the active site of the dephospho*Af*AGM1-GlcNAc6P is open, representing an inactive state of the enzyme while the phospho*Af*AGM1-GlcNAc-6P-Mg^{2+} adopts a semi-opened active site representing the active Michaelis complex. This complex however reveals that the mechanism of phosphoryl transfer from the active serine to the acceptor substrate might be due to the formation of an oxyanion of the 1-hydroxyl of GlcNAc-6P by proton uptake from *Af*AGM1_pSer69. Hence a mechanism of phosphoryl transfer involving the ionization of the acceptor substrate by the phosphate acting as the catalytic base is the most plausible mechanism. In conclusion, these enzymes suffer

large conformational changes, mainly in domain 4, which in turn are coupled to a precise phosphate-assisted mechanism in which phosphate may act as the catalytic base. The understanding of the catalytic mechanism can therefore be exploited in the rational design of a mechanism inspired inhibitors which are lacking for this class of enzymes.

Acknowledgment

The authors would like to thank the European Synchrotron Radiation Facility, Grenoble, for time on beamline BM14 and ID-14. This work was funded by the MRC Programme Grant M004139.

Table I: Details of data collection and structure refinement. Values between the brackets are for the highest resolution shell. All measured data were included in structure refinement.

	*Af*AGM1–GlcNAc-6P	*Af*AGM1_S69A-Glc-1,6-bisP
Resolution	20.00 (2.34)	20.00 (1.90)
Space group	$P2_12_12_1$	$P2_12_12_1$
Unit cell		
a (Å)	71.3	80.9
b (Å)	84.8	87.6
c (Å)	186.4	91.9
No. of reflections	183592	191366
No. of unique reflections	48393	51704
I/σ (I)	34.7 (1.8)	19.2 (2.7)
Completeness (%)	99.8	97.6
Redundancy	3.5 (3.9)	3.7 (3.6)
R_{merge} (%)	5.7 (66.6)	3.4 (48.2)
RMSD from ideal geometry		
Bonds (Å)	0.010	0.012
Angles (°)	1.5	2.1
R_{work} (%)	21.0	16.0
R_{free} (%)	27.7	20.0
No. of mol. in a.s.u	2	1
No. of residues	1036	541
No. of water mol.	297	471
B factors (Å^2)		
Overall	52.4	26.9
Protein	52.6	26.3
Ligand	56.4	30.6
Solvent	48.2	31.9
PDB ID	5OAW	5O9X

Table II: Kinetic parameters of *Af*AGM1. The coupled assay with G6PDH (Figure 1) was used to measure *Af*AGM1 activity using Glc-1P as the substrate in the presence or absence of Glc-1,6-bisP. The colorimetric assay involving purified *Af*UAP1 or *Trypanosoma brucei* UDP-glucose pyrophosphorylase as coupling enzymes (Figure 1) was used to measure *Af*AGM1 activity using GlcNAc-6P or Glc-6P as the substrate respectively. The results are the mean ± SD for three determinations. ND: Not detectable. The values for the wild type enzyme have been reported earlier but are shown here for comparison purposes with *Af*AGM1_S69A and *Af*AGM1_S507A mutants [12].

Substrate	WT	S69A	S507A
Glc-1P			
K_m (μM)	1200 ± 100		1900 ± 100
V_{max} (μmol/s)	0.38 ± 0.01		0.138 ± 0.004
k_{cat} (s^{-1})	37.6	nd	13.8
Glc-1P + Glc-1,6P			
K_m (μM)	400 ± 30		1200 ± 100
V_{max} (μmol/s)	0.41 ± 0.01		0.121 ± 0.004
k_{cat} (s^{-1})	41.0	nd	12.1
GlcNAc-6P			
K_m (μM)	25 ± 8		25 ± 9
V_{max} (μmol/s)	0.021 ± 0.002	nd	0.008 ± 0.001
k_{cat} (s^{-1})	0.21		0.08
Glc-6P			
K_m (μM)	300 ± 48		2900 ± 600
V_{max} (μmol/s)	0.018 ± 0.001		0.011 ± 0.001
k_{cat} (s^{-1})	0.18	nd	0.11

FIGURE LEGENDS

Figure 1. **Schematic illustrations of *Af*AGM1 assays**. (A). Phosphoglucomutase assay; a coupled assay with glucose-6-phosphate dehydrogenase (G6PDH) using G-1P as substrate. (B). Phosphoglucosamine mutase assay; a coupled assay with *Aspergillus fumigatus* UDP-*N*-acetylglucosamine pyrophosphorylase (*Af*UAP1) and pyrophosphatase using GlcNAc-6P as substrate. (C). A reverse phosphoglucomutase assay; a coupled assay with *Trypanosoma brucei* UDP-glucose pyrophosphorylase (*Tb*UGP) and pyrophosphatase using G-6P as substrate.

Figure 2. Overall structure of *Af*AGM1. (A) Overall crystal structure of one of the two monomers found in the asymmetric unit of *Af*AGM1-GlcNAc-6P-Mg^{2+} ternary complex. Domains 1, 2, 3 and 4 are coloured in red, blue, green and brown, respectively. The carbon sticks of *Af*AGM1_pSer69 and GlcNAc-6P are coloured in yellow and grey, respectively. (B) Surface representation of the monomeric forms of *Af*AGM1 in complex with GlcNAc-6P and Glc-1,6-bisP that show different conformational states during catalysis (colours of the different domains are the same as above).

Figure 3. **Active sites of *Af*AGM1 and *Ca*AGM1 in complex with different ligands**. The active sites of *Af*AGM1-GlcNAc-6P-Mg^{2+} and *Af*AGM1_S69A-Glc-1,6-bisP complexes are compared with *Ca*AGM1-GlcNAc-6P-Zn^{2+}-phosphate (PDB 2DKC) and *Ca*AGM1-GlcNAc-1P-Zn^{2+}-phosphate (PDB 2DKD) complexes [2]. Carbon atoms of residues within the active site pocket and sugars are shown as grey and green sticks, respectively. Mg^{2+} and Zn^{2+} ions, and water molecules are shown as pink, yellow and blue spheres, respectively. Hydrogen bond interactions between the protein and the ligands are shown as black dashed lines while Mg^{2+} and Zn^{2+} co-ordinations are shown as brown dash lines. The $|F_o|$ - $|F_c|$, φ_{calc} electron density maps around the ligands are shown contoured at 2.5 σ also the final $2|F_o|$ - $|F_c|$ electron density map for the phosphorylated active Ser69 is shown, contoured at 1.0 σ. A black arrow indicates the in-line angle of attack of 158^o of 1-hydroxyl of GlcNAc-6P on the phosphate located in *Af*AGM1_pSer69.

Figure 4. Catalytic mechanism. (A) Model of wild type *Af*AGM1 active site in complex with Glc-1,6-bisP and magnesium. Colours are the same as Figure 3 and a hydrogen atom bound to Ser69 is shown in yellow. (B) Scheme of the proposed reaction mechanism of phosphoacetylglucosamine mutase.

Supplementary Figure 1. **Superposition of the different *Af*AGM1 conformations**. This reveals movements of domains 1 and 4, with domain 4 making the greater movement towards the active site cleft. (A). *Af*AGM1_S69A+Glc1,6-bisP (Closed conformation) and phospho*Af*AGM1_GlcNAc-6P+Mg^{2+} (semi-open) with an RMSD of 2.1 Å. (B). *Af*AGM1+GlcNAc-6P (Open conformation) and phospho*Af*AGM1 GlcNAc-6P+Mg^{2+} (semi-open conformation) with an RMSD of 0.76 Å and (C). *Af*AGM1+GlcNAc-6P (open) and *Af*AGM1_S69A+Glc1,6-bisP (closed conformations), RMSD 2.3 Å. Coloured green is semi-opened, purple is closed and blue is opened conformations respectively. Figures 1 to 4 indicates the position of the domains and black arrows are pointing to the moving loops.

Supplementary Figure 2. Video showing the different stages of conformational change. Again, the secondary structures of domains 1, 2, 3 and 4 are coloured in red, blue, green and brown, respectively and the domain 4 showing the greatest movement.

REFERENCES

1. Hofmann, M., Boles, E. & Zimmermann, F. K. (1994) Characterization of the essential yeast gene encoding N-acetylglucosamine-phosphate mutase, *Eur J Biochem.* **221**, 741-7.
2. Nishitani, Y., Maruyama, D., Nonaka, T., Kita, A., Fukami, T. A., Mio, T., Yamada-Okabe, H., Yamada-Okabe, T. & Miki, K. (2006) Crystal structures of N-acetylglucosamine-phosphate mutase, a member of the alpha-D-phosphohexomutase superfamily, and its substrate and product complexes, *J Biol Chem.* **281**, 19740-7.
3. Milewski, S., Gabriel, I. & Olchowy, J. (2006) Enzymes of UDP-GlcNAc biosynthesis in yeast, *Yeast.* **23**, 1-14.
4. Kuhn, H. M., Meier-Dieter, U. & Mayer, H. (1988) ECA, the enterobacterial common antigen, *FEMS Microbiol Rev.* **4**, 195-222.
5. Kabanov, D. S. & Prokhorenko, I. R. (2010) Structural analysis of lipopolysaccharides from Gram-negative bacteria, *Biochemistry (Mosc).* **75**, 383-404.
6. Lovering, A. L., Safadi, S. S. & Strynadka, N. C. (2012) Structural perspective of peptidoglycan biosynthesis and assembly, *Annu Rev Biochem.* **81**, 451-78.
7. Fujita, M. & Kinoshita, T. (2012) GPI-anchor remodeling: potential functions of GPI-anchors in intracellular trafficking and membrane dynamics, *Biochim Biophys Acta.* **1821**, 1050-8.
8. Schwarz, F. & Aebi, M. (2011) Mechanisms and principles of N-linked protein glycosylation, *Curr Opin Struct Biol.* **21**, 576-82.
9. Hart, G. W., Slawson, C., Ramirez-Correa, G. & Lagerlof, O. (2011) Cross talk between O-GlcNAcylation and phosphorylation: roles in signaling, transcription, and chronic disease, *Annu Rev Biochem.* **80**, 825-58.
10. Mio, T., Yabe, T., Arisawa, M. & Yamada-Okabe, H. (1998) The eukaryotic UDP-N-acetylglucosamine pyrophosphorylases. Gene cloning, protein expression, and catalytic mechanism, *J Biol Chem.* **273**, 14392-7.
11. Mio, T., Yamada-Okabe, T., Arisawa, M. & Yamada-Okabe, H. (1999) Saccharomyces cerevisiae GNA1, an essential gene encoding a novel acetyltransferase involved in UDP-N-acetylglucosamine synthesis, *J Biol Chem.* **274**, 424-9.
12. Fang, W., Du, T., Raimi, O. G., Hurtado-Guerrero, R., Marino, K., Ibrahim, A. F., Albarbarawi, O., Ferguson, M. A., Jin, C. & Van Aalten, D. M. (2013) Genetic and structural validation of Aspergillus fumigatus N-acetylphosphoglucosamine mutase as an antifungal target, *Biosci Rep.* **33**.
13. Griffin, J. L., Bowler, M. W., Baxter, N. J., Leigh, K. N., Dannatt, H. R., Hounslow, A. M., Blackburn, G. M., Webster, C. E., Cliff, M. J. & Waltho, J. P. (2012) Near attack conformers dominate beta-phosphoglucomutase complexes where geometry and charge distribution reflect those of substrate, *Proc Natl Acad Sci U S A.* **109**, 6910-5.
14. Jolly, L., Ferrari, P., Blanot, D., Van Heijenoort, J., Fassy, F. & Mengin-Lecreulx, D. (1999) Reaction mechanism of phosphoglucosamine mutase from Escherichia coli, *Eur J Biochem.* **262**, 202-10.
15. Levin, S., Almo, S. C. & Satir, B. H. (1999) Functional diversity of the phosphoglucomutase superfamily: structural implications, *Protein Eng.* **12**, 737-46.
16. Cheng, P. W. & Carlson, D. M. (1979) Mechanism of phosphoacetylglucosamine mutase, *J Biol Chem.* **254**, 8353-7.
17. Jolly, L., Pompeo, F., van Heijenoort, J., Fassy, F. & Mengin-Lecreulx, D. (2000) Autophosphorylation of phosphoglucosamine mutase from Escherichia coli, *J Bacteriol.* **182**, 1280-5.
18. Oesterhelt, C., Schnarrenberger, C. & Gross, W. (1997) The reaction mechanism of phosphomannomutase in plants, *FEBS Lett.* **401**, 35-7.

19. Baxter, N. J., Bowler, M. W., Alizadeh, T., Cliff, M. J., Hounslow, A. M., Wu, B., Berkowitz, D. B., Williams, N. H., Blackburn, G. M. & Waltho, J. P. (2010) Atomic details of near-transition state conformers for enzyme phosphoryl transfer revealed by MgF-3 rather than by phosphoranes, *Proc Natl Acad Sci U S A.* **107**, 4555-60.
20. Otwinowski, Z. & Minor, W. (1997) Processing of X-ray diffraction data collected in oscillation mode, *Methods in Enzymology.* **276**, 307.
21. Murshudov, G. N., Vagin, A. A. & Dodson, E. J. (1997) Refinement of macromolecular structures by the maximum-likelihood method, *Acta Crystallogr D Biol Crystallogr.* **53**, 240-55.
22. Emsley, P. & Cowtan, K. (2004) Coot: model-building tools for molecular graphics, *Acta Crystallogr D Biol Crystallogr.* **60**, 2126-32.
23. Schuttelkopf, A. W. & van Aalten, D. M. (2004) PRODRG: a tool for high-throughput crystallography of protein-ligand complexes, *Acta Crystallogr D Biol Crystallogr.* **60**, 1355-63.
24. DeLano, W. L. (2004) Use of PYMOL as a communications tool for molecular science, *Abstr Pap Am Chem S.* **228**, U313-U314.
25. Mok, M. T. & Edwards, M. R. (2005) Critical sources of error in colorimetric assay for UDP-N-acetylglucosamine pyrophosphorylase, *Anal Biochem.* **343**, 341-3.
26. Maestro9 (2009) Schrödinger, LLC, New York, NY.
27. Kaminski, G. A., Friesner, R. A., Tirado-Rives, J. & Jorgensen, W. L. (2001) Evaluation and Reparametrization of the OPLS-AA Force Field for Proteins via Comparison with Accurate Quantum Chemical Calculations on Peptides, *J Phys Chem B.* **105**, 6474–6487.
28. Regni, C., Schramm, A. M. & Beamer, L. J. (2006) The reaction of phosphohexomutase from Pseudomonas aeruginosa: structural insights into a simple processive enzyme, *J Biol Chem.* **281**, 15564-71.
29. Mio, T., Yamada-Okabe, T., Arisawa, M. & Yamada-Okabe, H. (2000) Functional cloning and mutational analysis of the human cDNA for phosphoacetylglucosamine mutase: identification of the amino acid residues essential for the catalysis, *Biochim Biophys Acta.* **1492**, 369-76.
30. Naught, L. E. & Tipton, P. A. (2001) Kinetic mechanism and pH dependence of the kinetic parameters of Pseudomonas aeruginosa phosphomannomutase/phosphoglucomutase, *Arch Biochem Biophys.* **396**, 111-8.
31. Naught, L. E., Regni, C., Beamer, L. J. & Tipton, P. A. (2003) Roles of active site residues in Pseudomonas aeruginosa phosphomannomutase/phosphoglucomutase, *Biochemistry.* **42**, 9946-51.
32. Regni, C., Naught, L., Tipton, P. A. & Beamer, L. J. (2004) Structural basis of diverse substrate recognition by the enzyme PMM/PGM from P. aeruginosa, *Structure.* **12**, 55-63.
33. Regni, C., Tipton, P. A. & Beamer, L. J. (2002) Crystal structure of PMM/PGM: an enzyme in the biosynthetic pathway of P. aeruginosa virulence factors, *Structure.* **10**, 269-79.
34. Hu, W., Sillaots, S., Lemieux, S., Davison, J., Kauffman, S., Breton, A., Linteau, A., Xin, C., Bowman, J., Becker, J., Jiang, B. & Roemer, T. (2007) Essential gene identification and drug target prioritization in Aspergillus fumigatus, *PLoS Pathog.* **3**, e24.
35. Durand, P., Golinelli-Pimpaneau, B., Mouilleron, S., Badet, B. & Badet-Denisot, M. A. (2008) Highlights of glucosamine-6P synthase catalysis, *Arch Biochem Biophys.* **474**, 302-17.

Figure 1

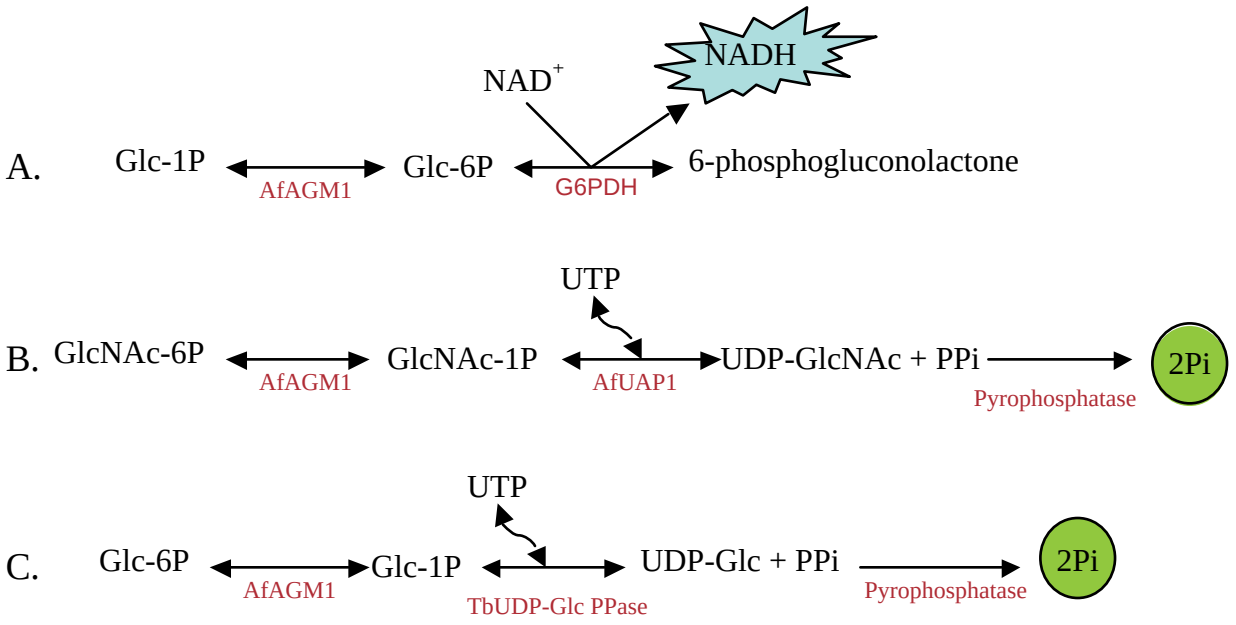
A.
Glc-1P
AfAGM1
Glc-6P
NAD+
NADH
G6PDH
6-phosphogluconolactone
B.
GlcNAc-6P
AfAGM1
GlcNAc-1P
UTP
AfUAP1
UDP-GlcNAc + PPi
Pyrophosphatase
2Pi
C.
Glc-6P
AfAGM1
Glc-1P
UTP
TbUDP-Glc PPase
UDP-Glc + PPi
Pyrophosphatase
2Pi

Figure 2

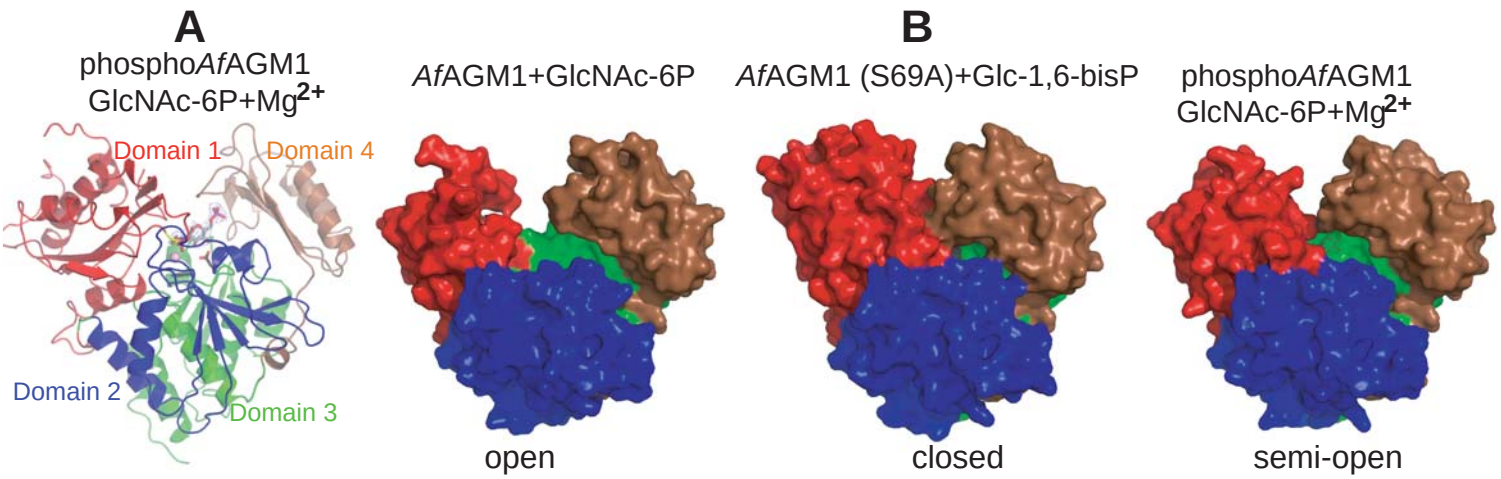
A
phospho*Af*AGM1
GlcNAc-6P+Mg2+
Domain 1
Domain 4
Domain 2
Domain 3
B
*Af*AGM1+GlcNAc-6P
*Af*AGM1 (S69A)+Glc-1,6-bisP
phospho*Af*AGM1
GlcNAc-6P+Mg2+
open
closed
semi-open

Phospho*Af*AGM1+ GlcNAc-6P + Mg^{2+}

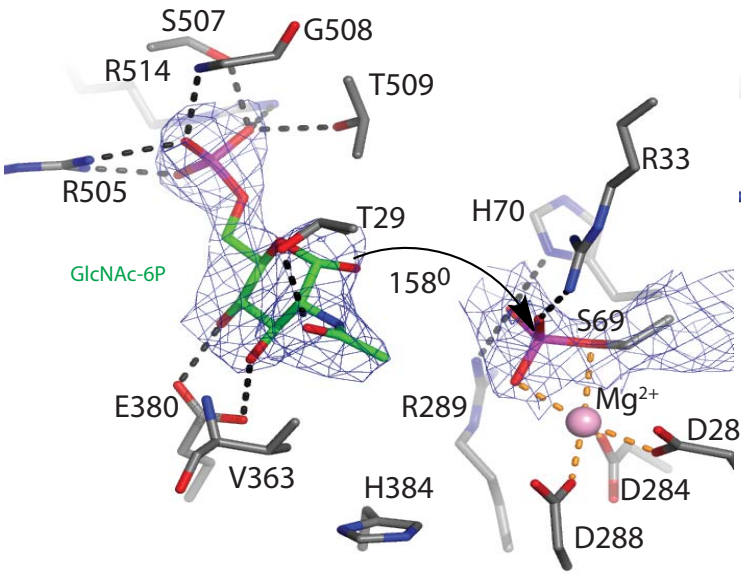

***Af*AGM1_S69A+Glc-1,6-bisP**

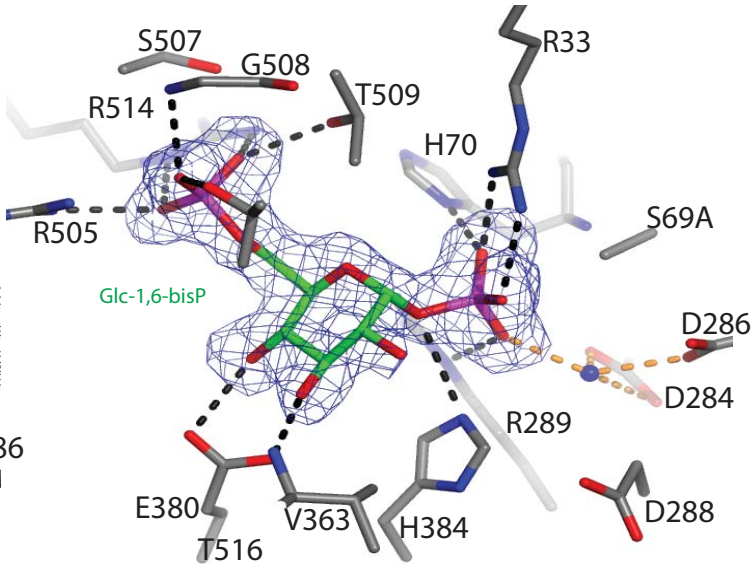

***Ca*AGM1+ GlcNAc-6P + Zn^{2+}**

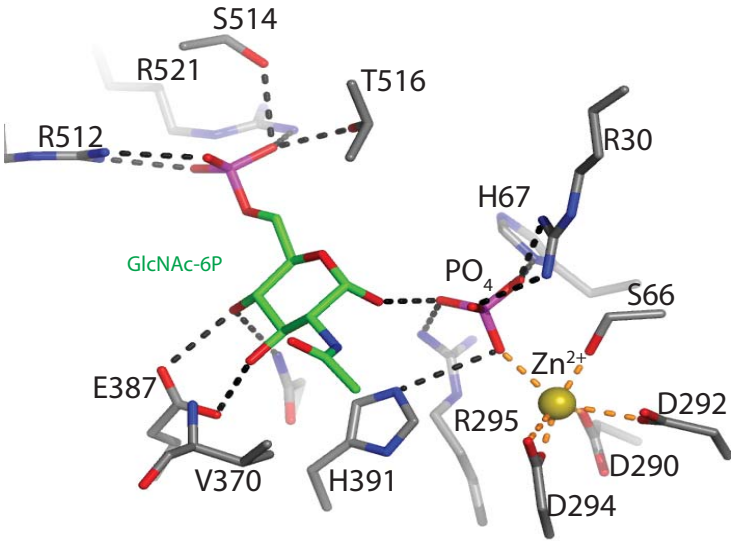

***Ca*AGM1 +GlcNAc-1P + Zn^{2+}**

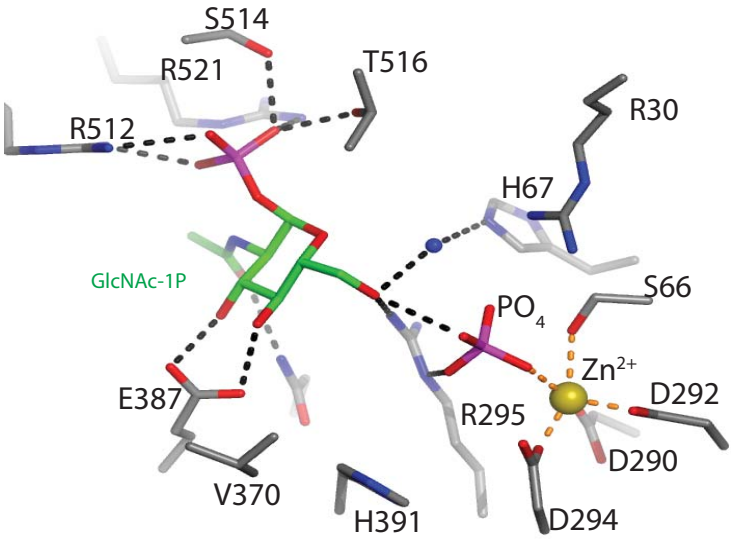

Figure 4

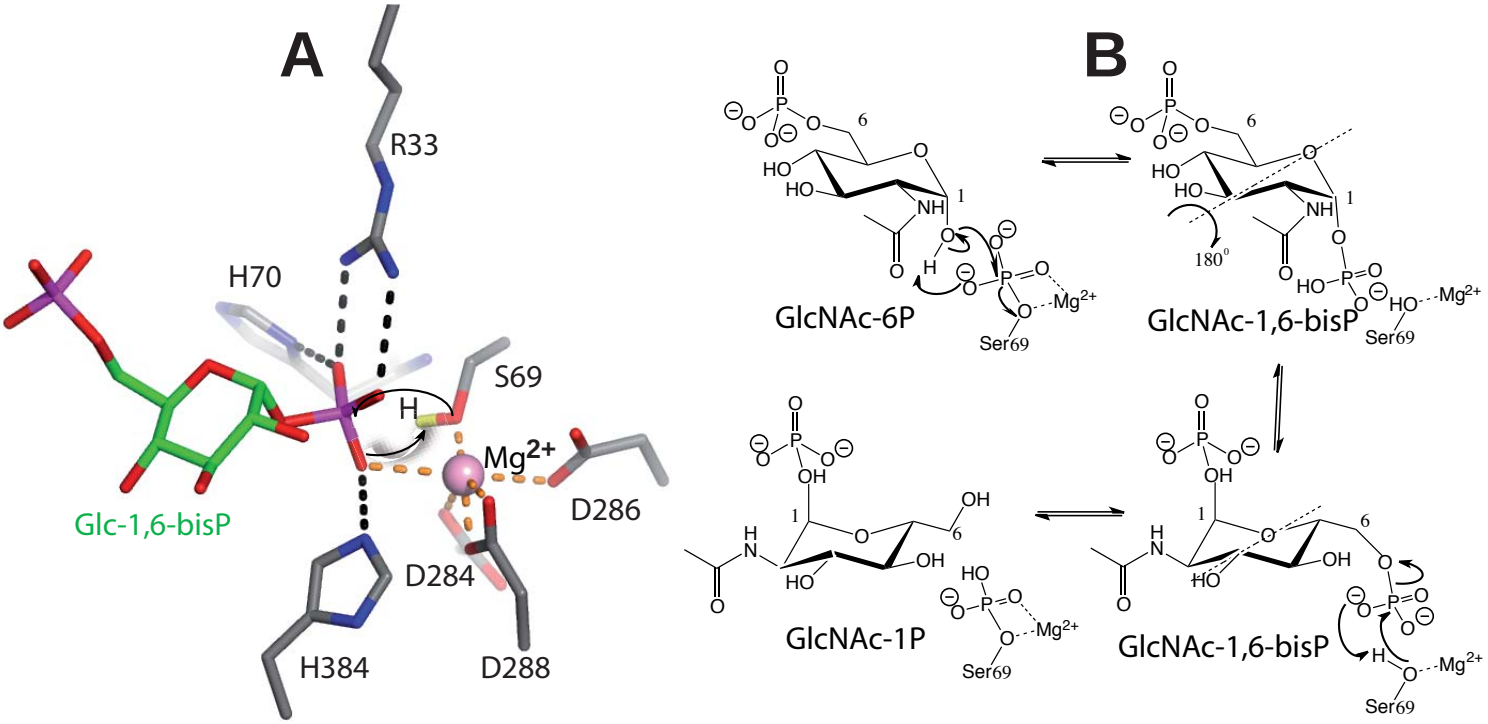
A
R33
H70
S69
H
Mg2+
D286
Glc-1,6-bisP
D284
H384
D288
B
GlcNAc-6P
Ser69
GlcNAc-1,6-bisP
Ser69
GlcNAc-1P
Ser69
GlcNAc-1,6-bisP
Ser69

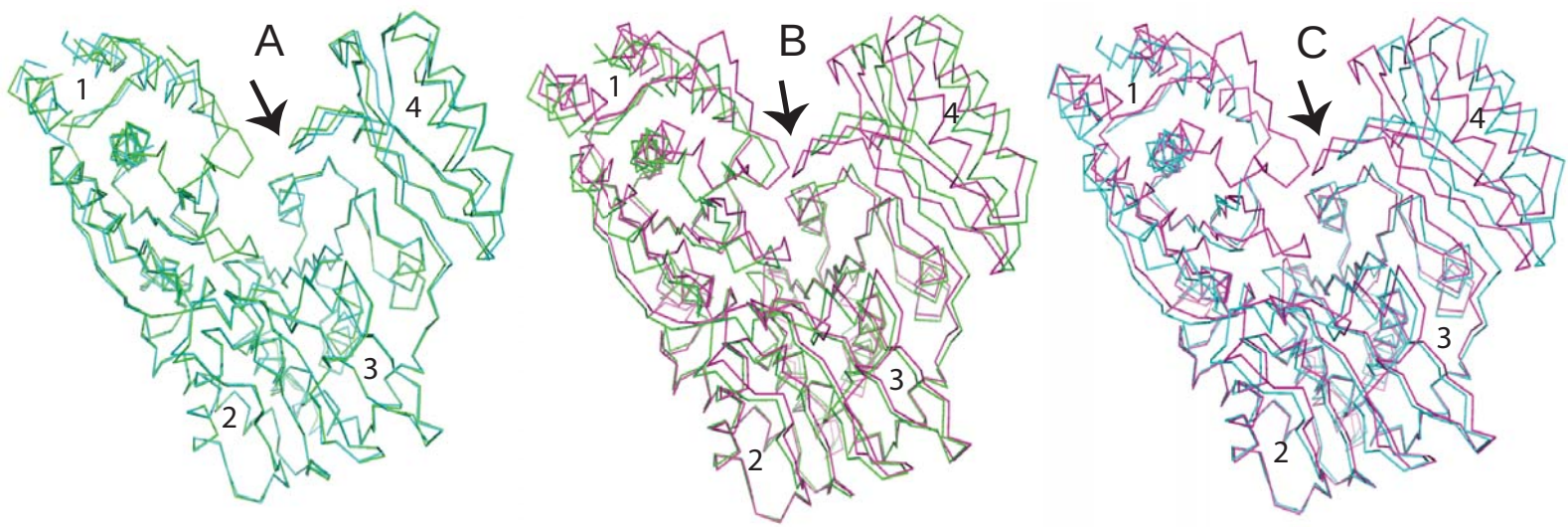
A
1
2
3
4
B
1
2
3
4
C
1
2
3
4